High-Dimensional Single-Photon Quantum Gates: Concepts and Experiments

Amin Babazadeh,[1,2,3] Manuel Erhard,[1,2,†] Feiran Wang,[1,2,4] Mehul Malik,[1,2] Rahman Nouroozi,[3] Mario Krenn,[1,2,*] and Anton Zeilinger[1,2]

[1]*Vienna Center for Quantum Science and Technology (VCQ), Faculty of Physics, University of Vienna, Boltzmanngasse 5, 1090 Vienna, Austria*

[2]*Institute for Quantum Optics and Quantum Information (IQOQI), Austrian Academy of Sciences, Boltzmanngasse 3, 1090 Vienna, Austria*

[3]*Physics Department, Institute for Advanced Studies in Basic Sciences (IASBS), Gavazang Road, Zanjan 45137-66731, Iran*

[4]*Key Laboratory of Quantum Information and Quantum Optoelectronic Devices, Shaanxi Province, Xi'an Jiaotong University, Xi'an 710049, China*

(Received 28 February 2017; revised manuscript received 4 July 2017; published 3 November 2017)

Transformations on quantum states form a basic building block of every quantum information system. From photonic polarization to two-level atoms, complete sets of quantum gates for a variety of qubit systems are well known. For multilevel quantum systems beyond qubits, the situation is more challenging. The orbital angular momentum modes of photons comprise one such high-dimensional system for which generation and measurement techniques are well studied. However, arbitrary transformations for such quantum states are not known. Here we experimentally demonstrate a four-dimensional generalization of the Pauli X gate and all of its integer powers on single photons carrying orbital angular momentum. Together with the well-known Z gate, this forms the first complete set of high-dimensional quantum gates implemented experimentally. The concept of the X gate is based on independent access to quantum states with different parities and can thus be generalized to other photonic degrees of freedom and potentially also to other quantum systems.

DOI: 10.1103/PhysRevLett.119.180510

Introduction.—High-dimensional quantum states have recently attracted increasing attention in both fundamental and applied research in quantum mechanics [1–5]. The possibility of encoding large amounts of information on a single photon makes them particularly interesting for large-alphabet quantum communication protocols [6–9] as well as for investigating fundamental questions concerning local realism or quantum contextuality [10,11]. The temporal and spatial structure of a photon provides a natural multimode state space in which to encode quantum information. The orbital angular momentum (OAM) modes of light [12] comprise one such basis of spatial modes that has emerged as a popular choice for experiments on high-dimensional quantum information [13]. While techniques for the generation and measurement of photonic qudits carrying OAM are well known [14–16], efficient methods for their control and transformation remain a challenge. No general recipe is known so far, and experimentally feasible techniques are known only for special cases.

Here we experimentally demonstrate a four-dimensional X gate and all of its integer powers with the orbital angular momentum modes of single photons. The four-dimensional X gate is a generalization of the two-dimensional σ_x Pauli transformation and acts as a cyclic ladder operator on a four-dimensional Hilbert space. The cyclic transformation required for this gate was designed through the use of the computer algorithm MELVIN [17], and the working principle of the cyclic transformation was demonstrated with laser light [18].

In particular, here we extend the conceptual idea of the X gate to a complete high-dimensional gate basis. Additionally, we present the experimental concept for the X^2 and $X^\dagger$ gate. Furthermore, we experimentally implement these three new gates at the quantum level. We show that these transformations work with a high quality on heralded single photons carrying orbital angular momentum as well as with coherent superpositions of OAM.

It is interesting to compare OAM with other high-dimensional degrees of freedom that allow for the encoding of quantum information. For path encoding, in particular, it is known how arbitrary single-qudit transformations can be performed in a lossless way [19]. Such transformations have been implemented recently on integrated photonic chips for the generation and transformation of entanglement [20,21]. General unitary transformations such as these are not known for the photonic OAM degree of freedom. In addition to being natural modes in optical communication systems with cylindrical symmetry, photons carrying OAM offer an important advantage over path and time-bin encoding in that quantum entanglement can be generated [22] and transmitted [23] without the need for interferometric stability. Therefore, the development of new controlled transformations for photonic OAM, as we show here, fills an important gap.

The X gate demonstrated here uses the ability to sort even and odd parity modes as a basic building block [24]. This concept can be extended to other photonic degrees of freedom such as frequency [25,26]. It will be interesting to see if our method can also be used in other proposed high-dimensional quantum systems such as trapped ions [27,28], cold atoms [29], and superconducting circuits [30] for constructing similar high-dimensional quantum logic gates.

High-dimensional Pauli gates.—The Pauli matrix group has applications in quantum computation, quantum teleportation, and other quantum protocols. This group is defined for a single qudit (a single photon with d-dimensional modes) in the following manner [31,32]:

$$X = \sum_{\ell=0}^{d-1} |\ell \oplus 1\rangle\langle\ell|, \tag{1a}$$

$$Z = \sum_{\ell=0}^{d-1} |\ell\rangle\omega^{\ell}\langle\ell|, \tag{1b}$$

where $\ell \in \{0, 1, \ldots, d-1\}$ refers to the different modes in the d-dimensional Hilbert space and $\ell \oplus 1 \equiv (\ell + 1) \bmod d$. The Z gate introduces a mode-dependent phase in the form of $\omega = \exp[(2\pi i/d)]$. Furthermore, the Y gate can be written $Y = XZ$. While the two-dimensional X gate swaps two modes with one another, in high-dimensional Hilbert spaces ($d > 2$) it takes the form of a cyclic operation:

$$X|\ell\rangle = |\ell \oplus 1\rangle. \tag{2}$$

This results in each state being transformed to its nearest neighbor in a clockwise direction, with the last state $|d-1\rangle$ being transformed back to the first one $|0\rangle$. The Y gate can be expressed as a combination of Z and X gates. While powers of Z lead to different mode-dependent phases, integer powers of X shift the modes by a larger number:

$$X^n = \sum_{\ell=0}^{d-1} |\ell \oplus n\rangle\langle\ell|. \tag{3}$$

The X^2 gate, for example, transforms each mode to the second nearest mode. Likewise, the conjugate of X leads to a cyclic operation in the counterclockwise direction:

$$X^{\dagger} = \sum_{\ell=0}^{d-1} |\ell \ominus 1\rangle\langle\ell|. \tag{4}$$

Using the Heisenberg-Weyl operators (following Ref. [33]), we can show that arbitrary unitary transformations can be achieved by a combination of X and Z gates and its integer powers (see Supplemental Material [34] for details). The Z gate for OAM qudits (the generalization of the two-dimensional σ_z Pauli transformation) introduces a mode-dependent phase, which can be implemented simply with a single optical element [24,35]. In the four-dimensional space, the here presented X, X^2, and $X^{\dagger}$ transformations in combination with Z, Z^2, and $Z^{\dagger}$ are sufficient for the construction of arbitrary unitary operations in a four-dimensional state space.

Experimental implementation.—A Z gate for photons carrying OAM can simply be achieved by using a dove prism, which has been shown recently [4,36–38]. Since the Y gate can be achieved by a combination of Z and X gates, it is sufficient to focus on the X gate and its powers. Figure 1(a) shows the schematic of the X gate. It consists of two parity sorters (PS1 and PS2) and a Mach-Zehnder interferometer (MZI) that is implemented between them. The input photon is first incident on a spiral phase plate that adds one quantum of OAM quantum ($\mathrm{SPP}_{\ell+1}$) onto the photon before it enters PS1. The parity sorter is an

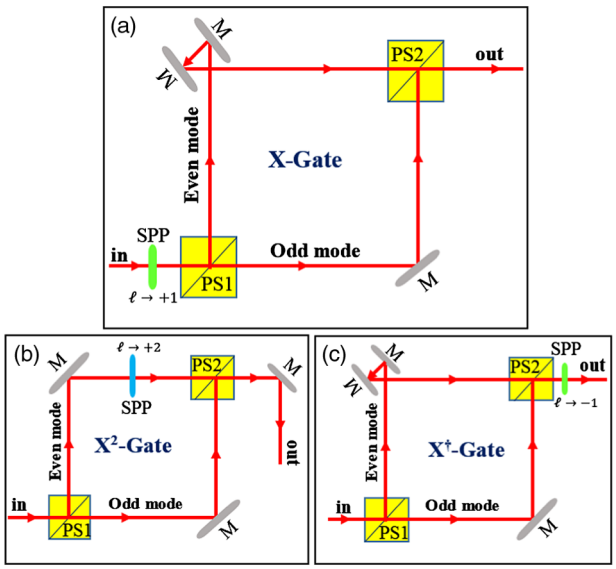

FIG. 1. The conceptual diagrams for the three types of quantum logic gates. The input states for each case is $(-2, -1, 0, 1)$. (a) A spiral phase plate (SPP) adds $+1$ to the mode, leading to $(-1, 0, 1, 2)$. Afterwards, the first parity sorter separates even and odd modes, while the second one combines them again—which forms a large interferometer. Within the interferometer, the even modes have an odd number of reflections, which leads to the correct output modes $(-1, 0, 1, -2)$. (b) For the X^2 gate, the input modes are directly separated into even and odd modes. After a reflection in each arm, the even modes are increased by 2. The two arms are recombined at the PS2, and all of the modes are reflected for changing the signs of the modes. That leads to $(0, 1, -2, -1)$. (c) In the $X^{\dagger}$ transformation, the different parity modes are separated again, and the even part gets reflected twice, while the odd modes are reflected once. After recombination, the ℓ of the modes is decreased by one, which leads to $(1, -2, -1, 0)$. Note that, in the experiment, it can be adjusted whether even or odd modes are reflected at the parity sorter. In this conceptual diagram, for simplicity we have chosen PS1 to reflect even modes and PS2 to reflect odd modes.

interferometric device which then sorts the photon according to its mode parity [24]. For the first-order cyclic transformation, the even-parity OAM mode undergoes a sign flip, while the sign of the odd-parity mode remains the same. This is achieved by reflecting the odd-parity mode at a mirror placed in one MZI path, while the even-parity modes undergo two reflections [see Fig. 1(a)]. The modes are then input into PS2, which coherently recombines them into the same path.

Fortuitously, the X gate has the very convenient property that it can be converted into the X^2 gate and $X^\dagger$ gate with only minor changes to the experimental setup (for $d = 4$, $X^\dagger = X^3$). This is beneficial in future implementations where quick, automated changes between gates are necessary (without physically moving optical components via the use of devices such as a spatial light modulator or a digital micromirror device). For constructing the X^2 gate, the $\mathrm{SPP}_{\ell+1}$ is removed and an $\mathrm{SPP}_{\ell+2}$ replaces the extra reflection in the even MZI path [Fig. 1(b)]. Changing the mode number within an interferometer is an important method used in many proposals for high-dimensional quantum transformation and entanglement creation techniques [17,39] and has not been experimentally demonstrated before. The $X^\dagger$ gate is achieved by simply moving the $\mathrm{SPP}_{\ell+1}$ from the input of PS1 and replacing it with an $\mathrm{SPP}_{\ell-1}$ at the output of PS2 [Fig. 1(c)].

The experimental setup is depicted in Fig. 2. We use heralded single photons produced via the process of type-II spontaneous parametric down-conversion process (SPDC) in a 5-mm-long periodically poled potassium titanyl phosphate (ppKTP) crystal pumped by a 405 nm diode laser. In the SPDC process, conservation of the pump angular momentum leads to the generation of photon pairs with a degenerate wavelength of $\lambda = 810$ nm that are entangled in OAM. Therefore, whenever the idler photon is measured to be in mode $|+\ell\rangle$, the signal photon is found to be in mode $|-\ell\rangle$. Thus, by heralding the idler photon in a particular OAM mode, we can select the OAM quantum number of the signal photon that is input into the logic gate. Here, we use the OAM quantum numbers of -2, -1, 0, and 1 for demonstrating our four-dimensional quantum logic gates. By changing the mode number before and after the transformation, the X gate can be used with every connected four-dimensional subspace.

The coherence length of heralded single photons from SPDC is several orders of magnitude smaller than that of the laser beam used in Ref. [18]. For this reason, we had to redesign the experiment to achieve the necessary long-term stability and control of path lengths: The parity sorter was originally proposed as an MZI with a dove prism in each arm [24]. The relative rotation angle between the two dove prisms is set at 90°, which introduces an $\ell\pi$ phase difference between the two arms. Depending on the parity of the OAM mode (ℓ) of the input photon, constructive or destructive interference results in even and odd modes

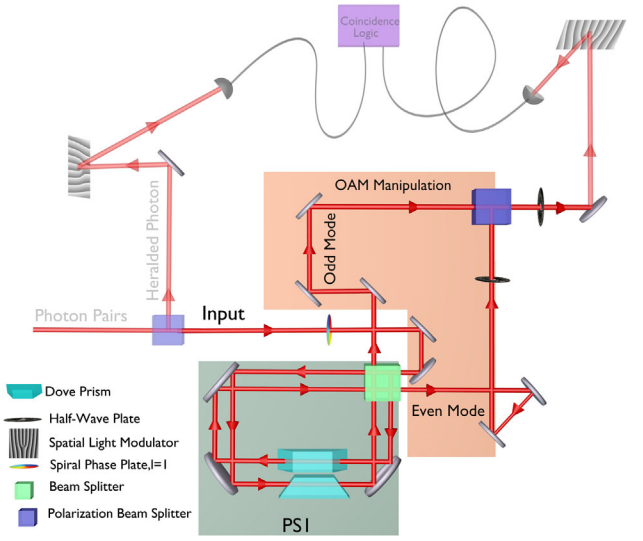

FIG. 2. Experimental setup for the four-dimensional X gate (additional experimental details are partially transparent). A 405 nm cw laser pumps a type-II ppKTP crystal (not shown), creating photon pairs entangled in OAM. The idler photon is used for heralding the signal photon in a particular OAM mode. After passing through a $\ell = +1$ spiral phase plate, the signal photon is input into a parity-sorting interferometer, which separates the odd and even OAM components of the photon. After traversing a series of mirrors, the odd and even components are coherently recombined in a Mach-Zehnder interferometer through the use of a polarizing beam splitter (PBS), a half-wave plate (HWP), and an effective polarizer (in the form of a SLM which acts only on horizontally polarized light). A spatial light modulator (SLM) and single mode fiber are used to perform projective measurements of OAM modes and their superpositions.

exiting different outputs of the MZI. For long-term stability, in our case we implement this interferometer in a double-path Sagnac configuration [40]. Two adjacent Sagnac loops allow for the positioning of a dove prism in each loop. The outputs of this Sagnac interferometer are then directly input into the second MZI (denoted as *OAM Manipulation* in Fig. 2). In the second interferometer, the sign of odd modes is flipped by reflection on an extra mirror. For the precise control of the relative path lengths, a trombone system in the odd arm is used to adjust the relative path difference to achieve a coherent combination of even and odd modes.

The concept of the quantum gates (discussed in Fig. 1) allows in principle for a lossless operation. For simplicity, we replace the second parity sorter with a polarization beam splitter (PBS). This allows the odd and even modes in the MZI to be recombined in a stable manner, albeit with an additional loss of 50%. As this loss is purely random, it does not change the OAM state of the transformed photon but only reduces its overall probability amplitude, i.e., the efficiency. Importantly, each detected photon is transformed correctly.

Now we explain the experimental details of the X gate (Figs. 1 and 2). A four-dimensional subset of OAM

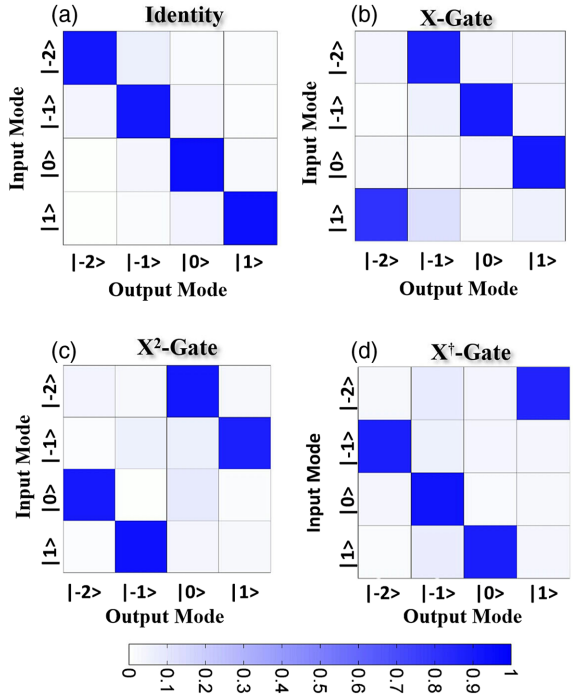

FIG. 3. Data showing the operation of the (a) identity, (b) X gate, (c) X^2 gate, and (d) $X^\dagger$ gate on the four-dimensional set of input states $\{|-2\rangle, |-1\rangle, |0\rangle, |1\rangle\}$. Each row shows the measured normalized coincidence rate in every output mode for a given input mode. The X gate implements a clockwise cyclic transformation $(-2 \to -1 \to 0 \to 1 \to -2)$, the X^2 gate swaps the odd and even modes $(-1 \leftrightarrow 1, -2 \leftrightarrow 0)$, and the $X^\dagger$ gate performs a counterclockwise cyclic transformation $(1 \leftarrow -2 \leftarrow -1 \leftarrow 0 \leftarrow 1)$. The average transformation efficiency for the X, X^2, and $X^\dagger$ gates are 87.3%, 90.4%, and 88.4%, respectively.

modes $\ell \in \{-2, -1, 0, 1\}$ is shifted by one leading to $\{-1, 0, 1, 2\}$. The parity sorter separates even and odd modes. The path for the even modes experiences an odd number of reflections that causes a sign flip and results in $\{-1, 0, 1, -2\}$. The coherent combination at the PBS and subsequent erasure of polarization information completes the X gate: $(-2 \to -1 \to 0 \to 1 \to -2)$. The X^2 and $X^\dagger$ gates work similarly; see Fig. 1. The experimental results of the gate operations are depicted in Fig. 3. The probability $P_{i,j}$ to detect a photon in mode j when sending in one in mode i is given by $P(i,j) = (|\langle j_{\text{out}}|i_{\text{in}}\rangle|^2 / \sum_n |\langle n_{\text{out}}|i_{\text{in}}\rangle|^2)$. The average probability of the expected mode for the X, X^2, and $X^\dagger$ gates is 87.3%, 90.4%, and 88.4%, respectively; see Table I. The lower detection probability for the X gate in the input mode $|1\rangle$ stems mainly from spatial misalignments which led to a lower coupling efficiency for this specific mode to the single photon detector.

In order to demonstrate a transformation of a coherent superposition, we use a four-dimensional input state for the gates. For that, we project the heralding photon with an equal superposition of $|T\rangle = |-2\rangle + |-1\rangle + |0\rangle + |1\rangle$, which triggers the input photon ideally into $|\psi\rangle = \alpha|-2\rangle + \beta|-1\rangle + \gamma|0\rangle + \delta|1\rangle$ (where $\alpha = 0.27$, $\beta = 0.47$, $\gamma = 0.7$, and $\delta = 0.46$). We measured the input state as ρ_{in}. Then we calculate the overlap between the expected state $\sigma_{\text{exp}} = A\rho_{\text{in}}A^\dagger$ (where A stands for the transformation X, X^2, $X^\dagger$) and measured state σ_{out} of the gate as $F_A(\rho_{\text{in}}, \sigma_{\text{out}}) = \text{Tr}(\sqrt{\sqrt{\sigma_{\text{exp},A}}\sigma_{\text{out}}\sqrt{\sigma_{\text{exp},A}}})$. We find experimentally that

$$\begin{aligned} F_X &= 93.4 \pm 0.9, \\ F_{X^2} &= 94.1 \pm 0.7, \\ F_{X^\dagger} &= 91.6 \pm 0.7, \end{aligned} \tag{5}$$

which shows that all three gates work with high quality in a coherent way. These results are possible only if all possible superpositions are transformed coherently.

An interesting question is how to compare these results with a *classical* gate. We suggest an intuitively appealing model, which is a measure-and-resend-based protocol, which we explain in detail in Supplemental Material [34]. We find that the maximal overlap F for the classical gate is bounded by $F_{\text{cl}} = 0.59$ for our input state. All of our experimental results are significantly above this bound.

Conclusion.—We have shown the experimental generation of the four-dimensional X gate and all of its unique higher orders, including the X^2 and X^3 gates. Together with the well-known Z gate, this forms a complete basis of transformations on a four-dimensional quantum system. This means that it can, in principle, be used to construct every four-dimensional unitary operation. The X gate is a basic element required for generating large classes of entangled states, such as the set of four-dimensional Bell states [41] or general high-dimensional multiparticle states [5,42]. Such states can be used, for example, in tests of

TABLE I. The probabilities $P_{i,j}$ to detect a photon in mode $|j\rangle$ for an input state $|i\rangle$. They are calculated by dividing the number of photons in the correct output state by the total number of counts measured in all four states. Errors are calculated using Monte Carlo simulations assuming Poissonian counting statistics.

Input mode	$\|-2\rangle$	$\|-1\rangle$	$\|0\rangle$	$\|1\rangle$
X gate	$88.1 \pm 3.2\%$	$90.3 \pm 1.8\%$	$90.9 \pm 1.5\%$	$80.1 \pm 2.9\%$
X^2 gate	$90.8 \pm 2.7\%$	$87.1 \pm 2.1\%$	$90.3 \pm 1.5\%$	$93.4 \pm 1.6\%$
$X^\dagger$ gate	$85 \pm 3\%$	$87.6 \pm 1.9\%$	$92.6 \pm 0.9\%$	$88.4 \pm 1.7\%$

quantum contextuality [43] and for Bell-like tests of local realism in a higher-dimensional state space [10,44].

These quantum logic gates can find application in various high-dimensional quantum protocols, such as high-dimensional quantum key distribution [6,7,45,46] where transformations between mutually unbiased bases are necessary. Other applications could include multiparty secret sharing [8] or dense coding [47], where transformations between orthogonal sets of entangled states are required. In quantum computing where complete sets of quantum gates are necessary, high-dimensional quantum states allow for the efficient implementation of gates [48,49] and offer advantages in quantum error correction [50].

Interestingly, a high-dimensional generalization of the CNOT gate consists of a controlled-cyclic transformation [51]. In a polarization-OAM hybrid space, one can create a lossless three-, six-, and eight-dimensional generalization [17] of our method. An important next step is the construction of high-dimensional two-particle gates. This would allow the implementation of complex quantum algorithms such as quantum error correction in high dimensions [50].

The authors thank Marcus Huber for helpful discussions. This work was supported by the Austrian Academy of Sciences (ÖAW), the European Research Council (SIQS Grant No. 600645 EU-FP7-ICT), and the Austrian Science Fund (FWF) with SFB F40 (FOQUS) and FWF project CoQuS No. W1210-N16. F. W. was supported by the National Natural Science Foundation of China (NSFC Grant No. 11534008). M. M. acknowledges support from the Austrian Science Fund (FWF) through the START Project No. Y879-N27 and the joint Czech-Austrian project MultiQUEST (I 3053-N27 and GF17-33780L).

A. B., M. E., and F. W. contributed equally to this work.

*mario.krenn@univie.ac.at
†manuel.erhard@univie.ac.at

[1] M. Agnew, J. Leach, M. McLaren, F. Stef Roux, and R. W. Boyd, Tomography of the quantum state of photons entangled in high dimensions, Phys. Rev. A **84**, 062101 (2011).
[2] J. Romero, D. Giovannini, D. S. Tasca, S. M. Barnett, and M. J. Padgett, Tailored two-photon correlation and fair-sampling: A cautionary tale, New J. Phys. **15**, 083047 (2013).
[3] M. Krenn, M. Huber, R. Fickler, R. Lapkiewicz, S. Ramelow, and A. Zeilinger, Generation and confirmation of a (100×100)-dimensional entangled quantum system, Proc. Natl. Acad. Sci. U.S.A. **111**, 6243 (2014).
[4] Y. Zhang, F. S. Roux, T. Konrad, M. Agnew, J. Leach, and A. Forbes, Engineering two-photon high-dimensional states through quantum interference, Sci. Adv. **2**, e1501165 (2016).
[5] M. Malik, M. Erhard, M. Huber, M. Krenn, R. Fickler, and A. Zeilinger, Multi-photon entanglement in high dimensions, Nat. Photonics **10**, 248 (2016).
[6] S. Gröblacher, T. Jennewein, A. Vaziri, G. Weihs, and A. Zeilinger, Experimental quantum cryptography with qutrits, New J. Phys. **8**, 75 (2006).
[7] A. Sit *et al.*, High-dimensional intracity quantum cryptography with structured photons, Optica **4**, 1006 (2017).
[8] M. Smania, A. M. Elhassan, A. Tavakoli, and M. Bourennane, Experimental quantum multiparty communication protocols, npj Quantum Inf. **2**, 16010 (2016).
[9] C. Lee, D. Bunandar, Z. Zhang, G. R. Steinbrecher, P. Ben Dixon, F. N. C. Wong, J. H. Shapiro, S. A. Hamilton, and D. Englund, High-rate field demonstration of large-alphabet quantum key distribution, arXiv:1611.01139.
[10] A. Vaziri, G. Weihs, and A. Zeilinger, Experimental Two-Photon, Three-Dimensional Entanglement for Quantum Communication, Phys. Rev. Lett. **89**, 240401 (2002).
[11] Y. Cai, J.-D. Bancal, J. Romero, and V. Scarani, A new device-independent dimension witness and its experimental implementation, J. Phys. A **49**, 305301 (2016).
[12] L. Allen, M. W. Beijersbergen, R. J. C. Spreeuw, and J. P. Woerdman, Orbital angular momentum of light and the transformation of Laguerre-Gaussian laser modes, Phys. Rev. A **45**, 8185 (1992).
[13] M. Krenn, M. Malik, M. Erhard, and A. Zeilinger, Orbital angular momentum of photons and the entanglement of Laguerre-Gaussian modes, Phil. Trans. R. Soc. A **375**, 20150442 (2017).
[14] A. Mair, A. Vaziri, G. Weihs, and A. Zeilinger, Entanglement of the orbital angular momentum states of photons, Nature (London) **412**, 313 (2001).
[15] M. Mirhosseini, O. S. Magaña-Loaiza, C. Chen, B. Rodenburg, M. Malik, and R. W. Boyd, Rapid generation of light beams carrying orbital angular momentum, Opt. Express **21**, 30196 (2013).
[16] M. P. J. Lavery, D. J. Robertson, G. C. G. Berkhout, G. D. Love, M. J. Padgett, and J. Courtial, Refractive elements for the measurement of the orbital angular momentum of a single photon, Opt. Express **20**, 2110 (2012).
[17] M. Krenn, M. Malik, R. Fickler, R. Lapkiewicz, and A. Zeilinger, Automated Search for New Quantum Experiments, Phys. Rev. Lett. **116**, 090405 (2016).
[18] F. Schlederer, M. Krenn, R. Fickler, M. Malik, and A. Zeilinger, Cyclic transformation of orbital angular momentum modes, New J. Phys. **18**, 043019 (2016).
[19] M. Reck, A. Zeilinger, H. J. Bernstein, and P. Bertani, Experimental Realization of Any Discrete Unitary Operator, Phys. Rev. Lett. **73**, 58 (1994).
[20] C. Schaeff, R. Polster, M. Huber, S. Ramelow, and A. Zeilinger, Experimental access to higher-dimensional entangled quantum systems using integrated optics, Optica **2**, 523 (2015).
[21] J. Carolan *et al.*, Universal linear optics, Science **349**, 711 (2015).
[22] J. Romero, D. Giovannini, S. Franke-Arnold, S. M. Barnett, and M. J. Padgett, Increasing the dimension in high-dimensional two-photon orbital angular momentum entanglement, Phys. Rev. A **86**, 012334 (2012).

[23] M. Krenn, J. Handsteiner, M. Fink, R. Fickler, and A. Zeilinger, Twisted photon entanglement through turbulent air across Vienna, Proc. Natl. Acad. Sci. U.S.A. **112**, 14197 (2015).
[24] J. Leach, M. J. Padgett, S. M. Barnett, S. Franke-Arnold, and J. Courtial, Measuring the Orbital Angular Momentum of a Single Photon, Phys. Rev. Lett. **88**, 257901 (2002).
[25] S. Yokoyama, R. Ukai, S. C. Armstrong, C. Sornphiphatphong, T. Kaji, S. Suzuki, J.-i. Yoshikawa, H. Yonezawa, N. C. Menicucci, and A. Furusawa, Ultra-large-scale continuous-variable cluster states multiplexed in the time domain, Nat. Photonics **7**, 982 (2013).
[26] Z. Xie *et al.*, Harnessing high-dimensional hyperentanglement through a biphoton frequency comb, Nat. Photonics **9**, 536 (2015).
[27] A. Muthukrishnan and C. R. Stroud, Jr., Multivalued logic gates for quantum computation, Phys. Rev. A **62**, 052309 (2000).
[28] A. B. Klimov, R. Guzman, J. C. Retamal, and C. Saavedra, Qutrit quantum computer with trapped ions, Phys. Rev. A **67**, 062313 (2003).
[29] A. Smith, B. E. Anderson, H. Sosa-Martinez, C. A. Riofrio, Ivan H. Deutsch, and Poul S. Jessen, Quantum Control in the cs 6 s 1/2 Ground Manifold Using Radio-Frequency and Microwave Magnetic Fields, Phys. Rev. Lett. **111**, 170502 (2013).
[30] M. Hofheinz *et al.*, Synthesizing arbitrary quantum states in a superconducting resonator, Nature (London) **459**, 546 (2009).
[31] D. Gottesman, in *Quantum Computing and Quantum Communications* (Springer, New York, 1999), pp. 302–313.
[32] J. Lawrence, Mutually unbiased bases and trinary operator sets for n qutrits, Phys. Rev. A **70**, 012302 (2004).
[33] A. Asadian, P. Erker, M. Huber, and C. Klöckl, Heisenberg-Weyl observables: Bloch vectors in phase space, Phys. Rev. A **94**, 010301 (2016).
[34] See Supplemental Material at http://link.aps.org/supplemental/10.1103/PhysRevLett.119.180510 for the proof of how to construct arbitrary unitaries with the Z and X gates including their integer powers and details on the model how to compare classical and quantum gates.
[35] A. N. De Oliveira, S. P. Walborn, and C. H. Monken, Implementing the deutsch algorithm with polarization and transverse spatial modes, J. Opt. B **7**, 288 (2005).
[36] M. Agnew, J. Z. Salvail, J. Leach, and R. W. Boyd, Generation of Orbital Angular Momentum Bell States and Their Verification via Accessible Nonlinear Witnesses, Phys. Rev. Lett. **111**, 030402 (2013).
[37] X.-L. Wang, X.-D. Cai, Z.-E. Su, M.-C. Chen, D. Wu, L. Li, N.-L. Liu, C.-Y. Lu, and J.-W. Pan, Quantum teleportation of multiple degrees of freedom of a single photon, Nature (London) **518**, 516 (2015).
[38] R. Ionicioiu, Sorting quantum systems efficiently, Sci. Rep. **6**, 25356 (2016).
[39] M. Krenn, A. Hochrainer, M. Lahiri, and A. Zeilinger, Entanglement by Path Identity, Phys. Rev. Lett. **118**, 080401 (2017).
[40] M. Erhard, M. Malik, and A. Zeilinger, A quantum router for high-dimensional entanglement, Quantum Sci. Technol. **2**, 014001 (2017).
[41] F. Wang, M. Erhard, A. Babazadeh, M. Malik, M. Krenn, and A. Zeilinger, Generation of the complete four-dimensional Bell basis, arXiv:1707.05760.
[42] M. Erhard, M. Malik, M. Krenn, and A. Zeilinger, Experimental GHZ entanglement beyond qubits, arXiv:1708.03881.
[43] R. Lapkiewicz, P. Li, C. Schaeff, N. K. Langford, S. Ramelow, M. Wieśniak, and A. Zeilinger, Experimental non-classicality of an indivisible quantum system, Nature (London) **474**, 490 (2011).
[44] A. C. Dada, J. Leach, G. S. Buller, M. J. Padgett, and E. Andersson, Experimental high-dimensional two-photon entanglement and violations of generalized Bell inequalities, Nat. Phys. **7**, 677 (2011).
[45] M. Mafu, A. Dudley, S. Goyal, D. Giovannini, M. McLaren, M. J. Padgett, T. Konrad, F. Petruccione, N. Lütkenhaus, and A. Forbes, Higher-dimensional orbital-angular-momentum-based quantum key distribution with mutually unbiased bases, Phys. Rev. A **88**, 032305 (2013).
[46] M. Mirhosseini, O. S. Magaña-Loaiza, M. N. O'Sullivan, B. Rodenburg, M. Malik, M. P. J. Lavery, M. J. Padgett, D. J. Gauthier, and R. W. Boyd, High-dimensional quantum cryptography with twisted light, New J. Phys. **17**, 033033 (2015).
[47] A. Hill, T. Graham, and P. Kwiat, Hyperdense coding with single photons, Front. Opt. FW2B (2016).
[48] T. C. Ralph, K. J. Resch, and A. Gilchrist, Efficient Toffoli gates using qudits, Phys. Rev. A **75**, 022313 (2007).
[49] B. P. Lanyon, M. Barbieri, M. P. Almeida, T. Jennewein, T. C. Ralph, K. J. Resch, G. J. Pryde, J. L. O'brien, A. Gilchrist, and A. G. White, Simplifying quantum logic using higher-dimensional Hilbert spaces, Nat. Phys. **5**, 134 (2009).
[50] A. Bocharov, M. Roetteler, and K. M. Svore, Factoring with qutrits: Shor's algorithm on ternary and metaplectic quantum architectures, Phys. Rev. A **96**, 012306 (2017).
[51] J. C. Garcia-Escartin and P. Chamorro-Posada, A swap gate for qudits, Quantum Inf. Process. **12**, 3625 (2013).